A unified solution to the small scale problems of the ΛCDM model II: introducing parent-satellite interaction

Antonino del Popolo, Morgan Le Delliou

Prepared for submission to JCAP

A unified solution to the small scale problems of the ΛCDM model II: introducing parent-satellite interaction

A. Del Popolo,[a,b,c] **M. Le Delliou**[d]

[a]Dipartimento di Fisica e Astronomia, University Of Catania, Viale Andrea Doria 6, 95125 Catania, Italy

[b]INFN sezione di Catania, Via S. Sofia 64, I-95123 Catania, Italy

[c]International Institute of Physics, Universidade Federal do Rio Grande do Norte, 59012-970 Natal, Brazil

[d]Instituto de Fisica Teorica IFT-UNESP, Rua Dr. Bento Teobaldo Ferraz 271, Bloco 2 - Barra Funda, 01140-070 São Paulo, SP Brazil

E-mail: adelpopolo@oact.inaf.it, delliou@ift.unesp.br

Abstract. We continue the study of the impact of baryon physics on the small scale problems of the ΛCDM model, based on a semi-analytical model (Del Popolo, 2009). With such model, we show how the cusp/core, missing satellite (MSP), Too Big to Fail (TBTF) problems and the angular momentum catastrophe can be reconciled with observations, adding parent-satellite interaction. Such interaction between dark matter (DM) and baryons through dynamical friction (DF) can sufficiently flatten the inner cusp of the density profiles to solve the cusp/core problem. Combining, in our model, a Zolotov et al. (2012)-like correction, similarly to Brooks et al. (2013), and effects of UV heating and tidal stripping, the number of massive, luminous satellites, as seen in the Via Lactea 2 (VL2) subhaloes, is in agreement with the numbers observed in the MW, thus resolving the MSP and TBTF problems. The model also produces a distribution of the angular spin parameter and angular momentum in agreement with observations of the dwarfs studied by van den Bosch, Burkert, & Swaters (2001).

Keywords: cosmology: theory - large scale structure of universe - galaxies: formation

Contents

1 Introduction **1**

2 Solving the remaining small scale problems of ΛCDM **4**
2.1 Mass loss caused by tidal stripping and tidal heating 5
2.2 Evaluation of luminous satellites 7

3 Results and discussion **10**

4 Conclusions **13**

A Dynamics of the satellites. **19**
A.1 Dynamical friction 19
A.2 Mass loss 20
A.3 Tidal Heating 21

1 Introduction

The ΛCDM (cosmological constant and Cold Dark Matter) model of cosmology, while describing the observations of the Universe, its large scale structure and evolution very successfully (Spergel et al. 2003, Komatsu et al. 2011; Del Popolo 2007, 2013, 2014a), retains some problems in the description of structures at small scales (e.g., Moore 1994; Moore et al. 1999; Ostriker & Steinhardt 2003; Boylan-Kolchin, Bullock, and Kaplinghat 2011, 2012; Oh et al. 2011)[1]. These problems can be enumerated as a) the discrepancy between cuspy density profiles obtained in N-body simulations (Navarro, Frenk & White 1996, 1997 (NFW); Navarro 2010)[2] and the flat profiles of dwarf and Low Surface Brightness galaxies (Burkert 1995; de Blok, Bosma, & McGaugh 2003; Del Popolo 2009 (DP09); Cardone et al. 2011a, 2011b; Cardone & Del Popolo 2012; Del Popolo 2012a,b (DP12a, DP12b); Oh et al. 2010, 2011; Kuzio de Naray & Kaufmann 2011), coined as the cusp/core problem (hereafter CCP) (Moore 1994; Flores & Primak 1994;Ogiya & Mori, 2011,2014; Ogiya et al. 2014), or of Galaxy Clusters (Del Popolo 2014b; Del Popolo & Gambera 2000); b) the discrepancy between the large discs of observed spirals and the small discs obtained in Smooth Particle Hydrodynamics (SPH) simulations, referred to as the angular momentum catastrophe (AMC, van den Bosch, Burkert,& Swaters, 2001); c) the discrepancy between the number of predicted and observed subhaloes when running N-body simulations (Klypin et al. 1999; Moore et al. 1999)[3], dubbed the "missing satellite problem" (MSP).

Klypin et al. (1999), and Moore et al. (1999) noticed, in numerical simulations of galactic and cluster haloes, an excess of predicted subhaloes compared with observation. They had found $\simeq$ 500 satellites with circular velocities larger than Ursa-Minor and Draco,

[1] Other remaining problems for the ΛCDM model involve understanding dark energy: the cosmological constant fine tuning problem (Weinberg 1989; Astashenok, & Del Popolo 2012), and the "cosmic coincidence problem".

[2] Note that the NFW profile, initially considered a universal one, has been shown not to be so (e.g., Del Popolo 2010, 2011)

[3] That difference is larger than an order of magnitude in the Milky Way (MW)!

while the MW dwarf Spheroidals (dSphs) are well known to be far fewer (the Large and Small Magellanic Clouds, and 9 bright dSphs (Boylan-Kolchin, Bullock, and Kaplinghat 2012)). The problem was later confirmed in subsequent cosmological simulations (Aquarius, Via Lactea II (VL2), and GHALO simulations – Springel et al. 2008; Stadel et al. 2009; Diemand et al. 2007). Although insufficiently for a complete solution, it was alleviated with the discovery of the ultra-faint MW satellites (Willman et al. 2005; Belokurov 2006; Zucker 2006; Sakamoto & Hasegawa 2006; Irwin et al. 2007).

The MSP was recently enriched with an extra problem, spawned from the analysis of the Aquarius and the Via Lactea simulations. Simulated haloes produced $\simeq 10$ subhaloes (Boylan-Kolchin, Bullock, and Kaplinghat 2011, 2012) that were too massive and dense to be the host of the MW brightest satellites: while those ΛCDM simulations predicted in excess of 10 subhaloes with $V_{max} > 25$ km/s, the dSphs of the MW all have $12 < V_{max} < 25$ km/s. This discrepancy in the kinematics between simulations and the MW brightest dSphs (Boylan-Kolchin, Bullock, and Kaplinghat 2011, 2012), which is an extra problem of the MSP, has been dubbed the Too-Big-To-fail (TBTF) problem[4] (Ogiya & Burkert 2014).

Similarly to the solutions to other small scale problems, the resolution of the MSP can be classified as either cosmological or astrophysical solutions. Cosmological solutions modify either the power spectrum at small scales (e.g. Zentner & Bullock 2003), the constituent DM particles (Colin, Avila-Reese & Valenzuela 2000; Sommer-Larsen & Dolgov 2001; Hu, Barkana & Gruzinov 2000; Goodman 2000; Peebles 2000; Kaplinghat, Knox, & Turner, M. S. 2000) or the gravity theories, like $f(R)$ (Buchdahl 1970; Starobinsky 1980), $f(T)$ (see Ferraro 2012), and MOND (Milgrom 1983a,b).

Several different kinds of astrophysical solutions have been proposed. In one picture, the present-day dwarf galaxies could have been more massive in the past, and they were transformed and reduced to their present masses by strong tidal stripping (e.g., Kravtsov, Gnedin & Klypin 2004). Another very popular picture is based on suppression of star formation due to supernova feedback (SF), photoionization (Okamoto et al. 2008; Brooks et al. 2013 (B13)), and reionization. In particular, reionization can prevent the acquisition of gas by DM haloes of small mass, then "quenching" star formation after $z \simeq 10$ (Bullock, Kravtsov, & Weinberg 2000; Ricotti & Gnedin 2005; Moore et al. 2006). This would suppress dwarfs (dSphs) formation or could make them invisible. Another solution combines the change of central density profiles of satellites from cuspy to cored (Zolotov et al. 2012 (Z12); B13), which makes the satellites more subject to tidal stripping and even subject to being destroyed (Strigari et al. 2007; Peñarrubia et al. 2010 (P10)). Tidal stripping is enhanced if the host halo has a disc. Disc shocking due to the satellites passing through the disc produce strong tidal effects on the satellites, even stronger if the satellite has a cored inner profile. The astrophysical solutions based on the role of baryons in structure formation, are more easy to constrain than cosmological solutions, and moreover do not request one to reject the ΛCDM paradigm.

While it is not complicated to separately solve the MSP problem, and the TBTF problem with the recipes discussed above, a simultaneous solution of both problems in models of galaxy formation based on DM-only simulations of the ΛCDM model (Boylan-Kolchin, Bullock & Kaplinghat 2012)[5], is much more complicated.

[4] "Too big to fail", in the sense that the extra simulation satellites are too big, compared with MW satellites, to remain invisible.

[5] Note that, in the case of the TBTF problem, the excess of massive subhaloes in MW could disappear if satellites density profiles are modelled through Einasto's profiles, or if the MW's virial mass is $\simeq 8 \times 10^{11} M_{\odot}$

Previous attempts to find a simultaneous solution to the abundance problem of satellites (MSP), and to the TBTF problem were made by the above mentioned Z12, and B13. Z12 found a correction to the velocity in the central kpc of galaxies, $\Delta v_{\rm c,1kpc}$, that mimicked the flattening of the cusp due to SF and tidal stripping.

This correction, together with its subsequent destruction effects from the tidal field of the baryonic disc, and the identification of subhaloes that remain dark because of their inefficiency in forming stars due to UV heating, were then applied by B13 to the subhaloes of the VL2 simulation (Diemand et al. 2008). As a result, the number of massive subhaloes in the VL2 were brought in line with the number of satellites of MW and M31.

This work extends a previous paper (Del Popolo *et al.* 2014), enriched with the part of the model described in appendix A, and will chiefly focus on the latter problem (MSP). However, the model also carries the solution for the former two (CCP and AMC), from the part of the model developed in Del Popolo *et al.* (2014). In clear, it uses a semi-analytical model to account for the dynamical evolution of satellites. The model, originated in DP09 (and DP12a, b), is an improved spherical infall model already discussed by many authors (Gunn & Gott 1972; Fillmore & Goldreich 1984; Bertschinger 1985; Hoffman & Shaham 1985; Ryden & Gunn 1987; Henriksen & Widrow 1995, 1997, 1999; Henriksen & Le Delliou 2002; Le Delliou & Henriksen 2003; Le Delliou 2008; Ascasibar, Yepes & Gottlöber 2004; Williams, Babul & Dalcanton 2004; Le Delliou, Henriksen & MacMillan 2010, 2011a, 2011b)[6].

In the present paper, we follow the path opened by Z12 and B13, but we consider another mechanism than SF that is also better able to flatten the density profiles of satellites. Namely, we use a mechanism based on the exchange of energy and angular momentum from baryons clumps to DM through dynamical friction (DF) (El-Zant et al. 2001, 2004; Ma & Boylan-Kolchin 2004; Nipoti et al. 2004; Romano-Diaz et al. 2008, 2009; DP09; Cole et al. 2011; Inoue & Saitoh 2011). We use DP09 to calculate the flattening of isolated satellites through the mechanism based on DF. In order to study the effect of tidal stripping and heating on the satellites, we use a combination of the procedures from Taylor & Babul (2001) (TB01) with that from P10. Our model differs from the TB01 and P10 models because we use a semi-analytical model based on DF (combination coined hereafter TBP model). In addition to the difference in the cuspy to cored profile mechanism, already present in B13, our TBP based model is properly taking into account the tidal heating mechanism. Such tidal heating is not captured in the SPH simulations from which Z12 derive their correction (as stressed in Sect. 4 of B13), since, as they point out, this would require a very high resolution to be captured (Choi et al. 2009). Moreover, we properly take into account disk shocking while this is neglected in Z12[7]: we account for the effects of satellites passing through the host galaxy disc.

Finally, the Δv_c-$v_{\rm infall}$ correction that we find shows a clearer trend (see the discussion in the following section). This is due to the absence, in our case, of numerical effects present, and described, in Z12[8] are not present.

In summary, although in our model the profile flattening is calculated as in Del Popolo *et al.* (2014), here the procedure from the model of Taylor & Babul (2001) is included

instead of $\simeq 10^{12} M_\odot$ (Vera-Ciro et al. 2013; Di Cintio et al. 2013).

[6]Changes to the spherical collapse introduced by dark energy where studied in Del Popolo *et al.* 2013a; Del Popolo, Pace, & Lima 2013a, b.; Del Popolo et al. 2013b.

[7]B13 is based on Z12 results. In Z12, some haloes experienced disc shocking and were strongly disrupted. For this, they were considered outliers, and not used in the calculation in the Z12 correction.

[8]The fact that gas-rich satellites in Z12 are too rich is probably due to inefficient stripping in their SPH simulations.

to follow the dynamics of satellites and their interactions with the main halo, and to take into account the mass loss during substructure evolution due to tides and tidal heating (see also Del Popolo & Gambera 1997). Moreover, inasmuch as inspired by Z12 and B13 in substructure treatment, we escaped the limitations of their SPH and SPH-based treatment with semi-analytic methods, obtaining a better $v_c - v_{infall}$ relation and accessing the effects of tidal heating and disc shocking. Our model employs a novel combination of parent-satellite interaction through dynamical friction, UV heating and tidal stripping to obtain satellite numbers and angular spin parameter distributions in agreement with observations.

The paper is organised as follows. In Sect. 2, we describe how the MSP and TBTF problem can be solved simultaneously when baryonic physics is properly taken into account, extending a model that has been shown to solve also the CCP and AMC. Appendix A gives the detail of the modified model, compared with Del Popolo *et al.* (2014). Sect. 3 describes the results, including a discussion. Sect. 4 is devoted to conclusions.

2 Solving the remaining small scale problems of ΛCDM

As we use a model that solves the other problems, we will concentrate here on the problems regarding the number and mass of satellites. Several solutions have been proposed to the MSP and TBTF problems (Strigari et al. 2007; Simon & Geha 2007; Madau et al. 2008; Zolotov et al. 2012; Brooks & Zolotov 2012; Purcell & Zentner 2012; Vera-Ciro et al. 2012; Di Cintio et al. (2012); Wang et al. 2012). B13 proposed an interesting baryonic solution to those two problems: instead of running SPH simulations of different galaxies, they tried to introduce baryonic effects in large N-body dissipationless simulations, like the VL2, showing that the result obtained is in agreement with observations of MW and M31 satellites.

In the following, we will partly follow their steps to obtain the corrected circular velocities and distribution of VL2 satellites. The differences between our model and Z12 or B13 have been reported in the introduction.

In summary the method is based on the following ideas and is divided into two main phases:

1. In the first phase, the satellite is considered isolated, without interactions with the host halo, and the flattening of the density profile produced by baryonic physics is calculated (in particular, the lowering of the central mass of subhaloes) in the same fashion as in, e.g., Del Popolo *et al.* (2014) (see also Hiotelis & Del Popolo 2006, 2013, to have a semi-analytical description of halos growth.). In this paper we deliberately chose not to take account of SF and to concentrate on the model of baryonic clumps exchanging energy and angular momentum with DM through DF, since it has clearly been shown (Del Popolo, 2014c, Fig. 4) that in the mass (circular velocity) range of the dwarfs studied in the present paper, the former is less efficient in transforming cusps into cores than the latter. Del Popolo & Hiotelis (2014) compared also the result of the current model, adding SF, to the SPH simulations of Inoue & Saitoh (2012): the full model agrees with the results of Inoue & Saitoh (2012). There, the addition of SF does not alter the outcome significantly. This phase is originally described in DP09.

2. Then comes the second phase, when the satellite, no longer considered isolated, is now subject to the tidal field of the host halo, and finally accreted to it. The total central mass is further reduced by tidal stripping and heating. This can be expressed in terms of changes in the circular velocity, v_c, also proportional to the density. More

precisely, we calculate the difference in circular velocity, at 1 kpc, between the DM-only (hereafter DMO) satellites and those containing also baryons (hereafter DMB satellites), $\Delta v_{\rm c,1kpc} = v_{\rm c,DMO} - v_{\rm c,DMB}$, and starting with the same DM content in our semi-analytical model.

Then, the effects of baryon physics, that are not taken into account in N-body simulations and responsible of the flattening of the profile, are introduced in the VL2 simulation by correcting the central circular velocity of the satellites, calculating their mass loss and ascribing them stellar masses and luminosities.

In other words, we obtain an analytical correction, along a similar idea to Z12 but with a semi-analytical model, using tidal stripping and tidal heating (recall the latter to be absent in Z12) that mimics the effect of flattening of the cusp. To this we add other corrections (e.g., tidal destruction and UV heating effects on subhaloes) discussed in DP09 and apply them to the satellites of the VL2 simulation, following the same principles as B13.

We stress again that in our model: a) contrary to Z12 and B13, the density profile flattening is due to DF and not to SF; b) tidal heating and disc shocking are taken into account differently from Z12 and B13; c) our model does not suffer from the numerical effect producing "artificially" rich satellites in the Z12 simulations.

Since the second phase contains the new method we propose to solve the problems involving the number and mass of satellites, we give its description in what follows.

2.1 Mass loss caused by tidal stripping and tidal heating

The second phase considers the effects of the interaction between the main halo and the satellite.

We follow a combination of TB01 with P10 models' procedures that properly take into account tidal stripping and heating after infall to extract accurate v_{max} values. TB01 compared their model with high resolution simulations, while P10 checked theirs, in their Appendix A, through high resolution N-body simulations.

The TB01 model follows the merger history, growth of the interacting satellites and tracks the substructure evolution, taking into account the mass loss due to tidal stripping, tidal heating, as well as enhancement of stripping due to the disc, in the host halo. The P10 model is fundamentally based on TB01, however not including tidal heating. Our model assumes the same DM host halo NFW (Navarro, Frenk & White 1996) density profile as P10. It also neglects, as P10 and contrary to TB01, the effect of its baryonic bulge. The latter assumption is justified by the disc's much larger mass than the bulge's, and its 10 times larger density gradient than found in the bulge or the halo. Such gradient endows the disk with 100 times more heating efficiency on the satellites than the other components.

This semi-analytic model, indicated as TBP model, is described in Appendix A.

At this point we may put together the mass decrease in satellites due to phase 1 (core flattening due to interaction of baryonic clumps with DM), and that due to tidal stripping and heating.

In Fig. 1 we plot the difference in circular velocity at 1 kpc, and at $z = 0$, between the DMO and DMB satellites of our semi-analytic calculations. This difference, $\Delta v_{\rm c,1kpc} = v_{\rm c,DMO} - v_{\rm c,DMB}$, is due to the cumulative effects of the two phases of the model: a) the flattening from cuspy to cored of density profiles due to dynamical friction interaction between baryon clumps and DM, and b) tidal stripping and heating from the crossing of the satellite

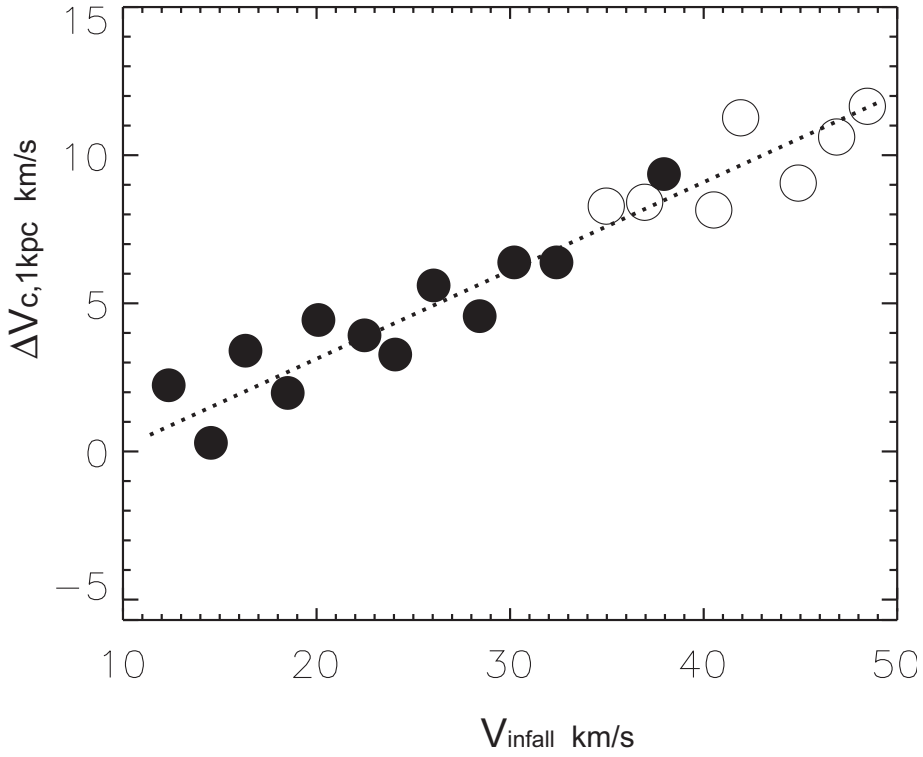

Figure 1. Difference in v_c at 1 kpc, and at $z = 0$, between DMO, and DMB satellites in terms of v_{max} of the DMO satellites at infall. The filled circles correspond to satellites with $M_b/M_{500} < 0.01$, while the open circles have $M_b/M_{500} > 0.01$.

through the host galaxy. The dashed line is a fit to the output points of the model, and is given by

$$\begin{aligned} \Delta(v_{1kpc}) &= 0.3\mathrm{v_{infall}} - 0.3\mathrm{km/s} \\ & 10\mathrm{km/s} < \mathrm{v_{infall}} < 50\mathrm{km/s} \end{aligned} \tag{2.1}$$

This correction is then applied to VL2 and is close to the results found by Z12 in the form

$$\begin{aligned} \Delta(v_{1kpc}) &= 0.2\mathrm{v_{infall}} - 0.26\mathrm{km/s} \\ & 20\mathrm{km/s} < \mathrm{v_{infall}} < 50\mathrm{km/s}. \end{aligned} \tag{2.2}$$

They obtained the above equation by fitting the output of their model, based on SF and tidal stripping, as displayed on their Fig. 8. Our Fig. 1 shows a clearer trend Δv_c-v_{infall}, as it doesn't suffer from the numerical effect, described in Z12 (see their Sect. 4 of B13), of inefficient stripping in SPH simulations.In addition, Z12 neglects disk shocking, as discussed in the introduction.These effects, properly taken into account in our model, explain the different results we obtain.

Equation 2.1, generated from our semi-analytical model, gives the difference between the equivalent of DM and enhanced SPH runs, and therefore the corrections to apply to satellites in N-body simulations to take account of the missing piece of baryonic physics.

In the case of $v_{infall} = 30$km/s, the Z12 correction gives $\Delta(v_{1kpc}) = 5.74$, while ours gives $\Delta(v_{1kpc}) = 8.7$. The difference between the two $\Delta(v_{1kpc})$ is due to the different models used to produce the pre-infall flattening of the satellites density profile and the tidal heating of subhaloes (Gnedin et al. 1999; Mayer et al. 2001; D'Onghia et al. 2010b; Kazantzidis et al. 2011).

Indeed, as stated, in Z12 the pre-infall flattening is due to SF, while in our case it is connected to DF. As shown by Cole et al. (2011), DF on infalling clumps is a very efficient mechanism in flattening the DM profile. On one hand, a clump having a mass of 1% of the halo mass can give rise to a core from a cuspy profile, removing twice its mass from the inner part of the halo. On another hand, the SF mechanism becomes less effective when going to lower masses: dwarfs with stellar mass $< 10^5 - 10^7 M_\odot$ have fewer stars and thus they contain, as a consequence, less supernovae explosions than dwarfs with stellar mass $> 10^7 M_\odot$ (Governato et al. 2012).

2.2 Evaluation of luminous satellites

The previous section exposed how baryonic corrections to dissipationless N-body simulations reduce the number of massive satellites. We are then left with the task to determine whether indeed the baryonic corrections also reduce the number of luminous satellites that are expected in dissipationless N-body simulations, and in particular to the satellites in VL2, and if this number is in agreement with those observed in the MW. In order to check this, other corrections are needed.

Our correction (Eq. 2.1), in the same way as the Z12 correction, produces satellites that reach $z = 0$ with their central v_c reduced by baryonic physics. However, some satellites are destroyed (by e.g. stripping or photo-heating) before $z = 0$. In N-body simulations, like the VL2, baryonic effects are not taken into account. In the real universe, or even SPH simulations, enhanced tidal stripping (due to the presence of a disc) may totally destroy some of the satellites seen in those N-body simulations. Our method requires then to determine the destroyed satellites before applying our Z12-inspired correction to VL2: to evaluate the luminous satellite population, we require the two following corrections: a) to account for the destruction by tidal stripping, and b) to account for suppression in star formation.

The first correction we apply to VL2 N-body satellites is the destruction rates by tidal stripping. For that, we need a relation between the mass retained since the infall and the change in the velocity (e.g., $v_{\rm max}$) in the same time interval.

We compute that relation applying our semi-analytical model, using the same satellites with which we calculated the relation $\Delta v_{\rm c,1kpc}$-$v_{\rm infall}$ (see DP09, appendix A, for the first phase). This population of satellites is split into three groups defined below.

We plot the result in Fig. 2. The filled circles represent the cored DMB satellites, having baryonic fraction $M_b/M_{500} > 0.01$, while the open circles show the cuspy DMB satellites, with baryonic fraction $M_b/M_{500} < 0.01$ (see Governato et al. (2012)). The open diamonds represent the DMO satellites.

The plot shows that DMB satellites loose more mass than DMOs. This can be explained by the following reasons: 1) DMB satellites contain gas, contrary to DMOs; 2) DMB satellites have flatter profiles than DMOs and thus suffer more tidal stripping (e.g., P10). The same

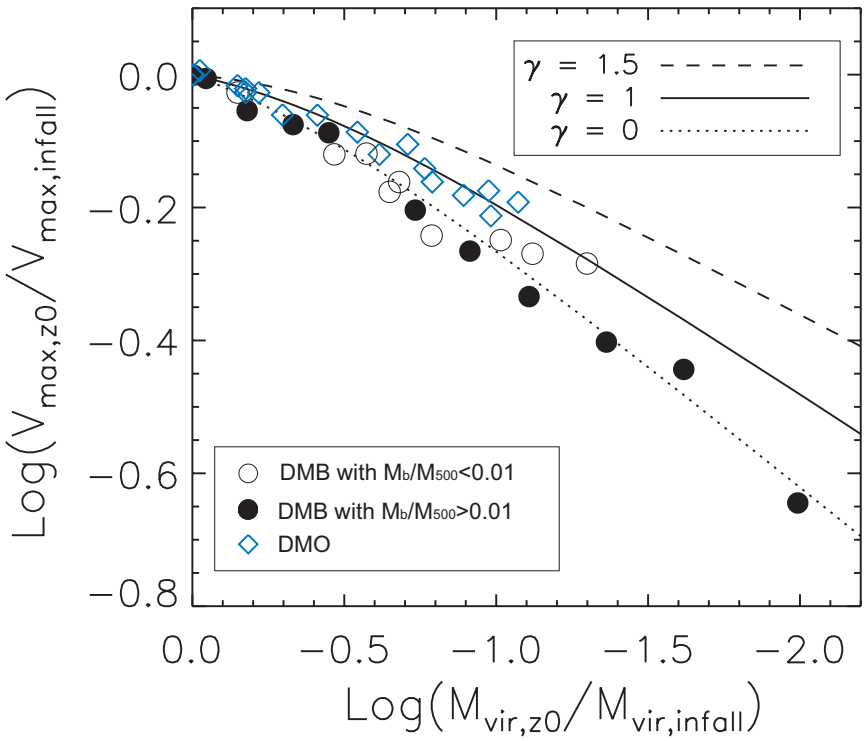

Figure 2. Change in the circular velocity at 1kpc between $z_{\rm infall}$ and $z = 0$ in terms of the retained mass. Filled circles represent the DMB satellites having baryonic fraction $M_b/M_{500} > 0.01$, while open circles, the DMB satellites with baryonic fraction $M_b/M_{500} < 0.01$. The open diamonds represent the DMO satellites. The dashed, solid, and dotted lines represents Eq. 8 of P10 for slope $\gamma = 1.5, 1, 0$, respectively.

goes between the baryon-richer DMB (filled circles) and baryon-poorer DMB (open circles). The maximum loss happen for DMB satellites in the vicinity of the host galaxy disc.

In Fig. 2, we also plot the analytic fits from Eq. 8 of P10 (see also their Fig. 6), describing the change in $v_{\rm max}$ as a function of mass lost due to tidal stripping

$$\frac{v_{\rm max}(z=0)}{v_{\rm infall}} = \frac{2^{\zeta} x^{\eta}}{(1+x)^{\zeta}} \tag{2.3}$$

where $x \equiv mass(z=0)/mass(z=infall)$.

The dashed line represents the above equation for central density profile logarithmic slopes $\gamma = 1.5$, that corresponds to $\zeta = 0.40$ and $\eta = 0.24$, the solid line stands for the case $\gamma = 1$, for which $\zeta = 0.40$ and $\eta = 0.30$, and the dotted line covers the case $\gamma = 0$, with $\zeta = 0.40$ and $\eta = 0.37$, respectively.

The $\gamma = 1$ curve in Fig. 2 gives a good fit to the change in $v_{\rm max}$ for the DMO satellites, and corresponds to cuspy density profiles. Conversely, the $\gamma = 0$ curve, that stands for cored profiles, presents a good approximation for the DMB satellites, particularly for those having large baryonic content (i.e., many stars).

Armed with the fit of Eq. (2.3), we propose to determine the VL2 satellites that are tidally disrupted by fixing a destruction criterion (e.g., mass lost). For satellites from N-

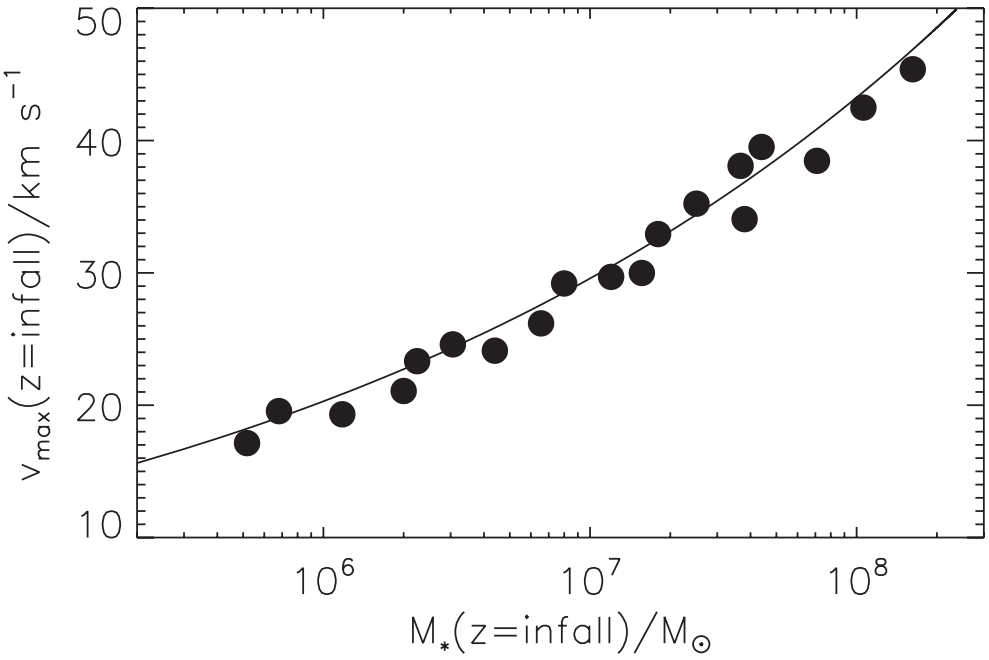

Figure 3. Values of $v_{\rm max}$ of the DMO subhaloes as function of the stellar mass, M_*, at infall. The solid line, the fit to the data given by $\frac{M_*}{M_\odot} = 0.1(\frac{v_{\rm infall}}{\rm kms^{-1}})^{5.5}$, indicates how stellar mass change with $v_{\rm infall}$.

body simulations, such as the VL2, inner slopes are expected at $\gamma \simeq 1$, as found in B13. Consequently, we fix for them $\zeta = 0.40$ and $\eta = 0.30$ in Eq. (2.3). The fit (2.3) enables to calculate the mass loss from VL2 satellites' velocities at infall and z=0 together with the infall mass. The velocity of VL2 satellites in the simulation at infall time, $v_{\rm c,VL2,infall}$, is modified with Phase 1 correction, $\Delta v_{\rm c,infall}$, to account for baryon flattening, yielding $v_{\rm max,infall} = v_{\rm c,VL2,infall} + \Delta v_{\rm c,infall}$. Using the correction from Eq. 2.1, the velocity of VL2 satellites in the simulation at present $v_{\rm c,VL2,z0}$ is modified into $v_{\rm max,z0} = v_{\rm c,VL2,z0} + \Delta v_{\rm c}$. The infall mass is directly obtained from the simulation $M_{\rm vir,infall} = M_{\rm sat,VL2}$.

As for the destruction criteria, we fix it similarly to B13, as follows. Tides affect much more cored, for which $\gamma = 0$, than cuspy satellites (with $\gamma = 1$). Governato et al. (2012) found that satellites having a stellar mass $> 10^7 M_\odot$, corresponding to $v_{\rm infall} > 30$ km/s, are cored, the opposite denoting a cusp. Here we assume, as B13 for our cuspy host with a disk and based on Fig. 2 in P10, that cored satellites, having $v_{\rm infall} > 30$ km/s, are disrupted if they loose $> 90\%$ of their mass after infall and pass at a distance < 20 kpc from the host galaxy centre. In the cases $v_{\rm infall} < 30$ km/s (cuspy satellite), or cored satellites with pericenters > 20 kpc, the halo is fully stripped off only if it loose 97% of its mass (Wetzel & White 2010).

Summarising, all the VL2 satellites loosing more than 97% mass ($x = 0.03$), or loosing more than 90% mass, combined with $v_{\rm infall} > 30$ km/s and a pericentric passages $< 20kpc$, are considered to be destroyed.

The second correction is the suppression of star formation by photo-heating, obtained from the Okamoto et al. (2008) results. In their paper, a uniform ionising background is assumed, for which He II reionization happens at $z = 3.5$, while it occurs at $z = 9$ for H and He I. They found the value of the typical halo mass retaining 50% of f_b: $M_t(z)$. This mass

can be converted into a typical velocity, $v_t(z)$[9]. Thus, if a VL2 subhalo has a larger peak velocity, $v_{\rm peak} > v_t$[10], it is considered to contain enough baryons to make it luminous.

The last step consists in assigning a luminosity to the surviving satellites. We first need to allocate stellar masses to VL2 satellites via a relation between their $v_{\rm infall}$ and the stellar mass M_*.

To do so, we recycled the pairs of satellites considered in the determination of $\Delta v_{\rm c,1kpc}$. DM-only subhaloes are usually associated with their DMB satellites at formation or accretion time (Bullock et al. 2000; Kravtsov et al. 2004; Strigari et al. 2007; Bovill & Ricotti 2011; Simha et al. 2012). Our semi analytical model simply creates a series of DMO, and a series of corresponding DMB haloes.

Fig. 3 plots $v_{\rm infall}$ in terms of the stellar mass, M_*. The $v_{\rm infall}$-M_* relation is obtained by fitting the data, yielding the relation[11]

$$\frac{M_*}{M_\odot} = 0.1(\frac{v_{\rm infall}}{\rm kms^{-1}})^{5.5}. \tag{2.4}$$

Finally, we need to relate M_* and the V-band magnitude, $M_{\rm V}$. We apply the relation from B13, extracted from Z12 simulations,

$$\log_{10}(\frac{M_*}{M_\odot}) = 2.37 - 0.38 M_{\rm V}. \tag{2.5}$$

3 Results and discussion

The result of the corrections discussed above are plotted in Fig. 4. The top panel represents the raw results from VL2 at $z = 0$. The bottom panel presents the results of applying the corrections discussed (heating, destruction, and velocity corrections) on the same satellites. The objects considered "observable" in the VL2 simulation are ascribed red filled symbols. Filled black circles are satellites that have lost $\geq$90% of their mass since infall, but do not satisfy the destruction criteria previously described: stripped of their stars, they actually appear much fainter than the "observable" ones (see P10, B13). Dark objects are marked by empty circles: simple empty circles have a mass smaller than the minimum to retain baryon and form stars, while objects crossed in addition with an "x", represent subhaloes that do not survive to the baryonic effects (e.g., baryonic disc, etc).

Note that the Z12 correction was not applied to satellites with $v_{max} > 50$km/s (for example, satellites with $M_V < -16$, the 5 most massive satellites at infall of VL2). In fact, those subhalos are Magellanic-like and gas-rich at accretion, possibly including an additional effect of adiabatic contraction that is not accounted for in the correction. The model also assumes small subhalo mass compared to the host. Therefore Magellanic-types are considered of a different dynamical nature and excluded from the model, as in, e.g. Simon & Geha (2007).

We obtain 3 satellites with $v_{1kpc} > 20$ km/s, in agreement with B13. However, our central velocities are smaller: the correction to the circular velocity, $\Delta(v_{1kpc})$, is larger in our model compared to Z12 and B13. In addition, in our case, some satellites are "overcorrected": their corrected velocities are negative.

[9] In the conversion, we used an overdensity $200\rho_{\rm crit}$, and a WMAP3 cosmology (Spergel et al. 2007).

[10] $v_{\rm peak}$ (see Del Popolo & Gambera 1996 for a definition of the peak mass) represents the largest value of $v_{\rm max}$ over the entire history of the subhalo.

[11] Note that tidal stripping and heating from $z_{\rm infall}$ to $z = 0$ produces a reduction in the halo masses, introducing scatter in the $v_{\rm infall}$-M_* relation at infall.

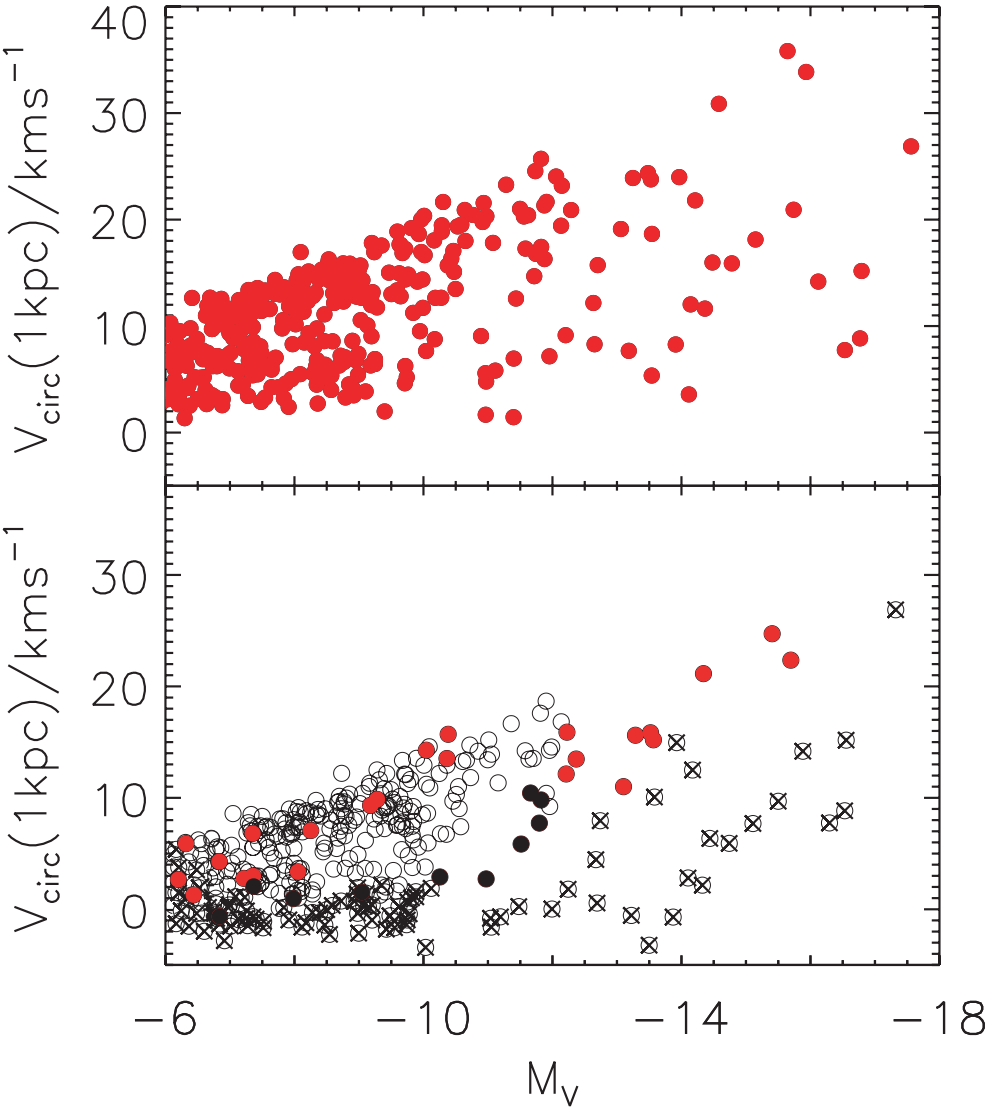

Figure 4. Plot of v_{1kpc} vs M_V for the VL2 simulation subhaloes. In the top panel, we plot the raw VL2 satellites velocities vs M_V at $z = 0$, as in B13. In the bottom panel, we present them after the baryonic corrections described in the text. The filled black circles represent satellites that have lost enough mass so that their stars are stripped and their luminosities are just upper limits, while their actual luminosities are much fainter at infall. Filled red circles are satellites actually observable at $z = 0$. Dark subhaloes are represented by empty circles, while circles with an x are subhaloes that have low probability to survive to tidal effects.

Similarly to B13, overcorrected haloes are part of a population that lost a great part of their mass after infall. At $z = 0$, their circular velocity at 1 kpc, v_{1kpc}, is very low so the correction $\Delta(v_{1kpc})$ brings them to negative values. After infall, that population suffers mass loss larger than 99.9% and exhibit tidal radii < 1 kpc. It can therefore be considered as a population of destroyed subhaloes.

It is interesting to note from Fig. 4 that the model obtains not only a reduction of the number of satellites, solving the MSP, but also a reduction of their central velocity, clearing up the TBTF problem.

In analogy with B13, UV heating and tidal destruction are necessary to reconcile the total number of luminous satellites with observations, while the Z12-type correction is necessary to reconcile the masses of the subhaloes with observations.

If the baryonic effects were not taken into account, a population would exist of satellites significantly more massive than those of the MW.

Finally, the effect of UV heating is required, in addition to tidal destruction, to get the correct number of luminous satellites.

In our model, the solution to the aforementioned problems is connected to the complex interaction between DM and baryons mediated by DF. Our study is similar to those of El-Zant et al. (2001, 2004), Romano-Diaz et al. (2008), Cole et al. (2011), in the sense that DF plays an important role. However, while previous studies considered one effect at a time (e.g., random angular momentum, angular momentum generated by tidal torques, adiabatic contraction, cooling, star formation), we consider the joint effect of all of them.

Indeed, here the dynamics of the satellites (i.e., the TBP model in Appendix A) proceeds from two competing mechanisms: dynamical friction, inducing a decay of the satellites orbits, and tidal stripping and heating, reducing the bound mass of the satellite. This reduction causes a decrease in the frictional force, which produces in turn a slowing down of the orbital collapse. Massive and dense satellite are more subject to DF and sink fast towards the centre of the potential. Low-density satellites are more subject to stripping and fall slowly towards the centre. Mass loss and tidal heating depend primarily on the satellite density profile, as confirmed by P10.

Accounting for tidal heating and disc shocking speeds up the disruption of satellite, and yields a further reduction of the mass retained by them compared with B13.

In Fig. 5, we compare the cumulative number of MW satellites in terms of the circular velocity of the halo with theoretical results. The upper solid line with diamonds represents the Via Lactea subhaloes (Diemand et al. 2007). The filled squares display the set of the sum of the classical MW dwarfs and the ultra-faint-dwarfs (Simon & Geha 2007). The dashed line shows the result of our model in terms of the abundance of subhaloes in the VL2 simulations after the baryonic corrections discussed. This figure is built superimposing our results, the dotted line, to those of Simon & Geha (2007) (their Fig. 14) in the V_c range 10 km/s-40 km/s. This is dictated by a) the fact that Eq. 2.1 is valid in the range $10 < V_{\rm infall} < 50$ km/s, so we considered satellites with $V_{\rm infall} > 10$ km/s; b) there are no halos at $z = 0$ that have circular velocities over 40 km/s. This plot demonstrates clearly how applying the baryonic correction to the VL2 subhaloes reduces the number of the satellites to reach the levels observed in the MW, thereby solving the MSP.

To solve the problem in a single galaxy is not enough to conclude that the problem is solved in galaxies different from ours. In fact, several authors have discussed the MSP in relation to the host galaxy mass. Di Cintio et al. (2012), Vera-Ciro et al. (2012), Wang et al. (2012), showed that if the MW true virial mass is smaller than $10^{12} M_\odot$, namely $\simeq 8 \times 10^{11} M_\odot$, the satellites excess may disappear. Since our model is not so computationally "heavy" as SPH simulations, it opens the door to study the MSP in different galaxies.

Summarising, the model shows how taking account of baryon physics allows to solve the small scale problems of the ΛCDM model.

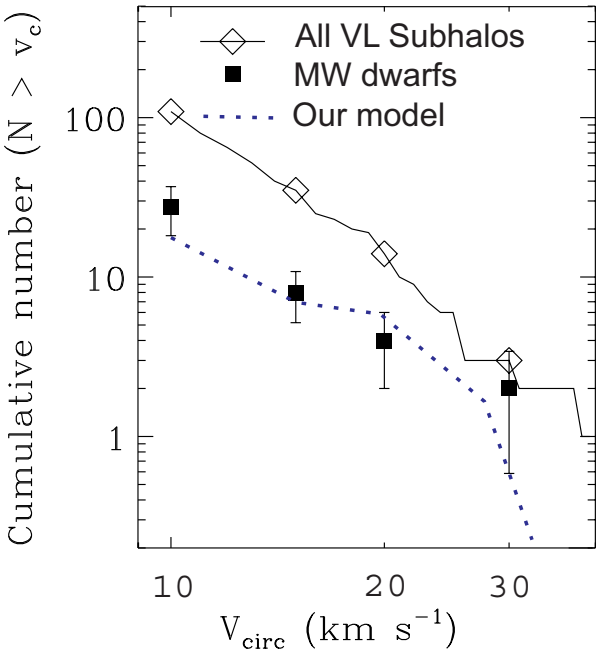

Figure 5. Cumulative number of MW satellites in terms of circular velocity. The filled squares display the classical MW plus ultra-faint-dwarfs in Simon & Geha (2007). The solid line with diamonds represents the abundance of the Via Lactea subhaloes (Diemand et al. 2007). The dashed line shows the abundance of subhaloes from VL2 after the baryonic corrections discussed in the text.

4 Conclusions

In the present paper, we looked for a common solution to the small scale problems of the ΛCDM using two semi-analytic models: a) the model presented in DP09 (see also DP12a, b) dealing with isolated satellites, and b) the model based on TB01, and P10 (TBP model) that involves satellite-host dynamics.

The study was divided into two phases: in the first, satellites were considered isolated and we studied, by means of the DP09 model, how the haloes profile are changed by adiabatic contraction, dynamical friction and the exchange of angular momentum, ordered and random, between baryons and DM. This applies both to isolated satellites and parent haloes alike, and solves the CCP (Del Popolo *et al.* 2014).

The model had already shown in DP09, DP12a,b, that the angular momentum generated through tidal torques and random velocities (random angular momentum) in the system, can be transferred in part to the DM from baryons through DF (Del Popolo *et al.* 2014). This produces a flattening of the cusp in agreement with previous studies based on DF (El-Zant et al. 2001, 2004; Romano-Diaz et al. 2008; Cole et al. 2011) and SF (Navarro et al. 1996a; Gelato & Sommer-Larsen 1999; Read & Gilmore 2005; Mashchenko et al. 2006, 2008).

In the second phase, satellites were allowed to interact with the host halo, and tidal stripping and heating were calculated through the TBP model.

We obtained a correction to the central velocity of the satellites from the cusp to core transformation before the satellites are accreted, and tidal stripping and heating produced from interaction with the main halo. This correction is close to that of Z12.

We then found the relation between the retained mass of satellites and the changes in $v_{\rm max}$ from $z_{\rm infall}$ to $z = 0$, and found a connection between mass loss and velocity change, in agreement with Eq. 8 of P10. This allowed us to determine the number of fully disrupted satellites because of tidal stripping and heating.

This correction, together with the effect of UV heating, and some criteria to fix which satellites are destroyed by tides, were applied to the VL2 satellites. As a result, the number of satellites is reduced and in agreement with the number observed in the MW. Similarly, the central velocity of satellites is reduced by the aforementioned corrections, suppressing the angular momentum catastrophe.

The present paper shows that baryonic physics is of fundamental importance to solve the small scale problems of the ΛCDM model: the MSP, the TBTF problem, the CCP (DP09), and the AMC (DP09). The possibility to solve those problems in the ΛCDM paradigm without the need to change the power spectrum or the constituent particles of DM is another proof of the robustness of the ΛCDM paradigm, and should, in addition, spur further studies in the direction followed in the present paper.

Acknowledgements

A.D.P. would like to thank the International Institute of Physics in Natal for the facilities and hospitality, Adi Zolotov, Alyson Brooks, and Charles Downing from Exeter University for a critical reading of the paper. The work of M.Le D. has been supported by FAPESP (2011/24089-5) and PNPD/CAPES20132029. M.Le D. also wishes to acknowledge IFT/UNESP.

References

[1] Arena S. E., Bertin G., 2007, A&A, 463, 921

[2] Ascasibar Y., Yepes G., Gottlöber S., 2004, MNRAS, 352, 1109

[3] Astashenok, A. V., and Del Popolo, A., 2012, Class. Quantum Grav. 29, 085014 (doi:10.1088/0264-9381/29/8/085014)

[4] V. Belokurov, V., ApJ 2006,, 647, L111-L114

[5] Bertschinger E., 1985, ApJS, 58, 39

[6] Bovill, M. S., & Ricotti, M. 2011, ApJ, 741, 17

[7] Boylan-Kolchin, M., Bullock, J. S., Kaplinghat, M, 2011, MNRAS 415L, 40

[8] Boylan-Kolchin, Michael; Bullock, James S.; Kaplinghat, Manoj, 2012, MNRAS 422, 1203

[9] Brooks A. M., & Zolotov, A., 2012, arXiv: 1207.2468

[10] Brooks, Alyson M.; Kuhlen, Michael; Zolotov, Adi; Hooper, Dan, 2013, ApJ 765, 22 (B13)

[11] Buchdahl, H. A., 1970, MNRAS, 150, 1-8.

[12] Bullock, J. S., Kravtsov, A. V., & Weinberg, D. H. 2000, ApJ, 539, 517

[13] Burkert, A. 1995, ApJ, 447, L25

[14] Cardone, V. F., Leubner, M.P., Del Popolo, A., 2011a MNRAS 414, 2265

[15] Cardone, V. F., Del Popolo, A., Tortora, C., Napolitano, N.R. 2011b, MNRAS 416, 1822

[16] Cardone, V. F., Del Popolo, A., 2012, MNRAS 427, 3176

[17] Chandrasekhar, S., 1943, ApJ 97, 255

[18] Choi, J.-H., Weinberg, M. D., & Katz, N. 2009, MNRAS, 400, 1247

[19] Colin, P., Avila-Reese, V., & Valenzuela, O. 2000, ApJ, 542, 622

[20] Cole, D. R., Dehnen,W., & Wilkinson, M. I. 2011, MNRAS, 416, 1118

[21] Colpi, M., Mayer, L., & Governato, F. 1999, ApJ, 525, 720

[22] D'Onghia, E., Vogelsberger, M., Faucher-Giguere, C.-A., & Hernquist, L. 2010b, ApJ, 725, 353

[23] de Blok, W. J. G., Bosma, A., & McGaugh, S. 2003, MNRAS, 340, 657

[24] Del Popolo, A., Gambera, M., 1996, A&A 308, 373

[25] Del Popolo, A., Gambera, M., 1997 A&A 321, 691

[26] Del Popolo, A., Gambera, M., 2000, A&A 357, 809

[27] Del Popolo, A., 2007, Astron. Rep., 51, 169

[28] Del Popolo, A., 2009, ApJ 698, 2093 (DP09)

[29] Del Popolo, A., 2010, MNRAS 408, 1808

[30] Del Popolo, A., 2011, JCAP 07, 014

[31] Del Popolo, A. & Kroupa, P., 2009A&A 502, 733

[32] Del Popolo, A., 2012a, MNRAS 424, 38 (DP12a)

[33] Del Popolo, A., 2012b, MNRAS 419, 971 (DP12b)

[34] Del Popolo, A., 2013, AIP Conference Proceedings 1548 , pp. 2-63

[35] Del Popolo, A., Cardone, V. F., & Belvedere, G., 2013a, MNRAS 429, 1080

[36] Del Popolo, A., Pace, F., Maydaniuk, S. P., Lima, J. A. S., Jesus, J. F., 2013b, Phys. Rev D, vol. 87, Issue 4, id. 043527

[37] Del Popolo, A., Pace, F., Lima, J. A. S., 2013a, MNRAS 430, 628

[38] Del Popolo, A., Pace, F., Lima, J. A. S., 2013b, IJMPD 22, 1350038

[39] Del Popolo, A., 2014a, IJMPD 23, 1430005

[40] Del Popolo, A. *et al.*, JCAP 04 (2014) 021

[41] Del Popolo, A., JCAP 07 (2014b) 019

[42] Del Popolo, A., Baltic Astronomy, 23 (2014c) 55

[43] Del Popolo, A., Hiotelis, N., JCAP 01 (2014) 047

[44] Di Cintio, A., Knebe, A., Libeskind, N. I., Brook, C., Yepes, G., Gottloeber, S., & Hoffman, Y. 2012, ArXiv e-prints

[45] Di Cintio, A., Knebe, A., Libeskind, N. I., Brook, C., Yepes, G., Gottlöber, S., Hoffman, Y., 2013, MNRAS 431, 1220-1229

[46] Diemand, J., et al. 2008, Nature 454, 735

[47] Diemand, J., Kuhlen, M., and Madau, P., 2007, ApJ 667, 859-877

[48] El-Zant A. A., Hoffman Y., Primack J., Combes F., Shlosman I., 2004, ApJ, 607, L75

[49] El-Zant, A., Shlosman, I., & Hoffman, Y. 2001, ApJ, 560, 636

[50] Ferraro, R., 2012, AIP Conf. Proc. 1471, 103-110, arXiv:1204.6273v2

[51] Fillmore J. A., Goldreich P., 1984, ApJ, 281, 1

[52] Flores R. A., Primack J. R., 1994, ApJ, 427, L1

[53] Gelato, S., & Sommer-Larsen, J. 1999, MNRAS, 303, 321

[54] Gnedin, O. Y., Hernquist, L., & Ostriker, J. P. 1999, ApJ, 514, 109

[55] Gnedin, O. Y., & Ostriker, J. P. 1997, ApJ, 474, 223

[56] Gnedin, O. Y., & Ostriker, J. P., 1999, ApJ, 513, 626

[57] Goodman, J. 2000, New Astron., 5, 103

[58] Governato, F., Zolotov, A., Pontzen, A., Christensen, C., Oh, S. H., Brooks, A. M., Quinn, T., Shen, S., Wadsley, J., 2012, MNRAS 422, 1231

[59] Gunn J. E., Gott J. R., 1972, ApJ, 176, 1

[60] Henriksen, R. N., Widrow, Lawrence M., 1995, MNRAS 276, 679

[61] Henriksen, R. N., Widrow, Lawrence M., 1997, Phys. Rev. Lett., 78, 3426

[62] Henriksen, R. N., Widrow, Lawrence M., 1999, MNRAS 302, 321

[63] Henriksen, R. N., Le Delliou M., 2002, MNRAS 331, 423

[64] Hiotelis, N., Del Popolo, A., 2006, Astrophys. Space Sci. 301, 67

[65] Hiotelis, N., Del Popolo, A., 2013, MNRAS 436, 163

[66] Hoffman Y., Shaham J., 1985, ApJ, 297, 16

[67] Hu,W., Barkana, R., & Gruzinov, A. 2000, Phys. Rev. Lett., 85, 1158

[68] Inoue, Shigeki; Saitoh, Takayuki R., 2012, MNRAS 422, 1902

[69] Inoue, Shigeki; Saitoh, Takayuki R., Mon. Not. R. Astron. Soc. 418, 2527-2531 (2011)

[70] Irwin, M. J., et al. 2007, ApJ, 656, L13

[71] Kaplinghat, M., Knox, L., & Turner, M. S. 2000, Phys. Rev. Lett., 85, 3335

[72] Kazantzidis, S., Lokas, E. L., Callegari, S., Mayer, L., & Moustakas, L. A., 2011, ApJ, 726, 98

[73] King, Ivan, 1962, AJ, 67, 274 and 565

[74] Klypin A., Kravtsov A. V., Valenzuela O., Prada, F., 1999, ApJ 522, 82

[75] Klypin A., Zhao H.-S., Somerville R. S., 2002, ApJ, 573, 597

[76] Komatsu, E., Smith, K. M., Dunkley, J., et al. 2011, ApJS, 192, 18

[77] Kravtsov, A. V., Gnedin, O. Y., & Klypin, A. A. 2004, ApJ, 609, 482

[78] Kundić , T., & Ostriker, J. P. 1995, ApJ, 438, 702

[79] Kuzio de Naray, R., Kaufmann, T., 2011, MNRAS.414.3617

[80] Le Delliou M., Henriksen R. N., 2003, A&A, 408, 27

[81] Le Delliou M., 2008, A&A, 490, L43-L48

[82] Le Delliou M., Henriksen R. N., MacMillan, J. D., 2010, A&A, 522, A28

[83] Le Delliou M., Henriksen R. N., MacMillan, J. D., 2011a, A&A, 526, A13

[84] Le Delliou M., Henriksen R. N., MacMillan, J. D., 2011b, MNRAS 413, 1633-1642

[85] Ma, C-P., Boylan-Kolchin, M., 2004, PhysRevLett 93, 021301

[86] Madau, Piero; Diemand, Jürg; Kuhlen, Michael, 2008, ApJ 679, 1260 -

[87] Mashchenko, S., Couchman, H. M. P., & Wadsley, J. 2006, Nature, 442, 539

[88] Mashchenko, S., Wadsley, J., & Couchman, H. M. P. 2008, Science, 319, 174

[89] Mayer, L., Governato, F., Colpi, M., et al. 2001, ApJ, 559, 754

[90] Milgrom, M., 1983a, ApJ 270, 365-370

[91] Milgrom, M. 1983b, ApJ 270, 371-389

[92] Moore B., 1994, Nat, 370, 629

[93] Moore, B., Quinn, T., Governato, F., Stadel, J., & Lake, G. 1999, MNRAS, 310, 1147

[94] Moore, B., Diemand, J., Madau, P., Zemp, M., & Stadel, J. 2006, MNRAS, 368, 563

[95] Navarro J. F. et al., 2010, MNRAS, 402, 21

[96] Navarro J. F., Frenk C. S., White S. D. M., 1996, ApJ, 462, 563

[97] Navarro, J. F., Eke, V. R., & Frenk, C. S. 1996a, MNRAS, 283, L72

[98] Navarro J. F., Frenk C. S., White S. D. M., 1997, ApJ, 490, 493

[99] Nipoti, C., Treu, T., Ciotti, L., Stavelli, M., 2004, MNRAS 355, 1119

[100] Ogiya & Mori, 2011, ApJ, 736, L2

[101] Ogiya & Mori, 2014, ApJ, 793, 46O

[102] Ogiya, Mori, Ishiyama, & Burkert, 2014, MNRAS, 440, L71

[103] Ogiya & Burkert, 2014, arXiv 1408.6444

[104] Oh, S-H, C. Brook, F. Governato, E. Brinks, L. Mayer,W. J. G. de Blok ,A. Brooks, F.Walter, 2010, AJ, 142, 24

[105] Oh, S-H, de Blok, W. J. G., Brinks, E., Fabian, W., Kennicutt, R. C., Jr., 2011 AJ 141, 193

[106] Okamoto, T., Gao, L., & Theuns, T. 2008, MNRAS, 390, 920

[107] Ostriker J. P., Steinhardt P., 2003, Science, 300, 1909

[108] Peebles, P. J. E. 2000, ApJ, 534, L127

[109] Peñarrubia, J., Just, A., Kroupa, P., 2004, MNRAS, 349, 747

[110] Peñarrubia, J., et al., 2010, MNRAS 406, 1290 (P10)

[111] Purcell, C. W., Zentner, A. R., 2012, JCAP 12, 007

[112] Quinn, P. J., & Goodman, J. 1986, ApJ, 309, 472

[113] Read, J. I., & Gilmore, G. 2005, MNRAS, 356, 107

[114] Ricotti, M., & Gnedin, N. Y. 2005, ApJ, 629, 259

[115] Romano-Diaz, E., Shlosman, I., Heller, C., & Hoffman, Y. 2009, ApJ, 702, 1250

[116] Romano-Diaz, E., Shlosman, I., Hoffman, Y., & Heller, C. 2008, ApJ, 685, L105

[117] Ryden B. S., Gunn J. E., 1987, ApJ, 318, 15

[118] Sakamoto, T., & Hasegawa, T. 2006, ApJ, 653, L29

[119] Simha, V., Weinberg, D. H., Davé, R., et al. 2012, MNRAS, 423, 3458

[120] Simon, J. D.; Geha, M., 2007, AAS 211, 2602

[121] Sommer-Larsen, J., & Dolgov, A. 2001, ApJ, 551, 608

[122] Spedicato, E., Bodon E., Del Popolo A., Mahdavi-Amiri N. 2003, 4OR, Vol. 1, Issue 1, 51

[123] Spergel, D. N., et al. 2007 ApJS 170 377 doi:10.1086/513700

[124] Spergel, D. N., Verde, L., Peiris, H. V., et al. 2003, ApJS, 148, 175

[125] Springel, V., Wang, J., Vogelsberger, M., Ludlow, A., Jenkins, A., Helmi, A., Navarro, J. F., Frenk, C. S., White, S. D. M., 2008, MNRAS 391, 1685

[126] Stadel J., Potter D., Moore B., Diemand J., Madau P., Zemp M., Kuhlen M., Quilis V., 2009, MNRAS, 398, 21

[127] Starobinsky, A. A. (1980). Physics Letters B 91: 99-102

[128] Stoehr, F., White, S. D. M., Tormen, G., & Springel, V. 2002, MNRAS, 335, L84

[129] Strigari, L. E., Bullock, J. S., Kaplinghat, M., Diemand, J., Kuhlen, M., Madau, P., 2007, ApJ 669, 676

[130] Taylor, J. E., Babul, A., 2001, ApJ 559:716-735

[131] van den Bosch F. C., Burkert A., Swaters R. A., 2001, MNRAS, 326, 1205 (VBS)

[132] van den Bosch, F. C., Lewis, G. F., Lake, G., & Stadel, J. 1999, ApJ, 515, 50

[133] Velazquez, Hector; White, Simon D. M., 1999, MNRAS, 304, 254

[134] Vera-Ciro, C. A., Helmi, A. Starkenburg, E., Breddels, M. A., 2013, MNRAS 428, 1696

[135] Wang, J., Frenk, C. S., Navarro, J. F., Gao, L., Sawala, T., 2012, MNRAS 424, 2715

[136] Weinberg, S., Rev. Mod. Phys., 1989, 61, 1

[137] Wetzel, A. R., & White, M. 2010, MNRAS, 403, 1072

[138] Williams, L. L. R., Babul, A., & Dalcanton, J. J. 2004, ApJ, 604, 18

[139] Willman, B., et al. 2005a, ApJ, 626, L85

[140] Zentner, A. R., & Bullock, J. S. 2003, ApJ, 598, 49

[141] Zolotov, A., Brooks, A. M., Willman, B., Governato, F., Pontzen, A., Christensen, C., Dekel, A., Quinn, T., Shen, S., Wadsley, J., 2012, ApJ 761, 71 (Z12)

[142] Zucker, D. B., et al. 2006a, ApJ, 643, L103

A Dynamics of the satellites.

In the following, we discuss a semi-analytic model that follows the substructure evolution within DM haloes. It takes into account the effects of DF, tidal loss and tidal heating. The model is basically the TB01 model with small changes coming from a similar model by P10.

Each satellite is represented by a spherically symmetric subhalo, whose structure is time dependent. At a time t, the satellite's state is specified by the form of the density distribution, from a chosen initial condition[12], by the mass bound to it, and by the heating experienced in time. For the determination of the satellite's orbit, we ignore its spatial extent and we solve its equation of motion in the potential of the host halo.

At each time step, the equations solved are:

$$\ddot{\mathbf{r}} = \mathbf{f}_h + \mathbf{f}_d + \mathbf{f}_{\rm df}; \tag{A.1}$$

In Eq. (A.1), the term $\mathbf{f}_h = -GM(<r)/r^2$ is the force due to the host halo, where

$$M(<r) = 4\pi \int_0^r \rho(r')r'^2 dr'; \tag{A.2}$$

and the density $\rho(r)$ is given by a NFW[13] profile with parameters $R_{\rm vir} = 258$ kpc, $r_s = 21.5$ kpc, $M_{\rm vir} = 10^{12} M_\odot$, and $\Delta_v = 101$ (Klypin et al. 2002; Peñarrubia et al. 2010). The term $\mathbf{f}_{\rm d}$ is the force produced by the baryonic disc. While in Peñarrubia et al. (2010) it is approximated by means of a Miyamoto-Nagai (1975) model, in Klypin et al. (2002) a double-exponential disc is used. We select the exponential disc applied in TB01, defined by the density

$$\rho_{\rm d}(r) = \frac{M_{\rm d}}{4\pi R_{\rm d}^2 z_0} exp(-\frac{R}{R_{\rm d}}) sech^2(\frac{z}{z_0}) \tag{A.3}$$

with $M_{\rm d} = 5.6 \times 10^{10} M_\odot$, $r_{\rm d} = 3.5$ kpc, and $z_0 = 700$ kpc. In this study, we neglect the bulge (similarly to P10), since the disc has a much larger mass than the bulge, and presents a steep vertical density gradient. That gradient is 10 times larger than for the bulge or the halo, resulting in satellite heating at disc crossing 100 times larger than from the other components.

A.1 Dynamical friction

The term $\mathbf{f}_{\rm df}$ is the dynamical friction force on the satellites due to the DM particles moving around the host. Dynamical friction is approximated through Chandrasekhar's formula (Chandrasekhar 1943) which is sufficiently accurate if one can consider the so called "Coulomb logarithm" as a free parameter, fixed through simulations (e.g., van den Bosch et al. 1999).

Chandrasekhar's formula, in our case is given by

$$\mathbf{f}_{\rm df} = \mathbf{f}_{\rm df,disc} + \mathbf{f}_{\rm df,halo} = -4\pi G^2 M_{sat}^2 \sum_{i=h,d} \rho_i(r) F(<v_{\rm rel,i}) \ln\Lambda_i \frac{\mathbf{v}_{\rm rel,i}}{v_{\rm rel,i}^3}. \tag{A.4}$$

having divided the potential into the halo and disc components. M_{sat} is the satellite mass, $\mathbf{r}$ its position, and $\ln\Lambda_h$ and $\ln\Lambda_d$ are the Coulomb logarithms of the halo and disc components,

[12] The initial density profile of the satellites is given by Appendix A.

[13] We recall that the NFW profile is given by $\rho(r) = \frac{\rho_s}{r/r_s(1+r/r_s)^2} = \frac{\rho_c \delta_v}{r/r_s(1+r/r_s)^2}$, where $\delta_v = \frac{\Delta_v}{3}\frac{c^3}{\log(1+c)-c/(1+c)}$ and ρ_c is the critical density. The scale radius r_s, and ρ_s depend on the formation epoch and are correlated with the virial radius of the halo, $R_{\rm vir}$, through the concentration parameter $c = R_{\rm vir}/r_s$.

respectively. If $\mathbf{v}_{sat}$ indicates the velocity vector of the satellite, then $\mathbf{v}_{\rm rel,h} = \mathbf{v}_{sat}$ is the satellite's relative velocity with respect to the halo, while $\mathbf{v}_{\rm rel,d} = \mathbf{v}_{sat} - \mathbf{v}_{d,\phi}$ the relative velocity with respect to the disc, while the term $v^2_{d,\phi} = R|f_d(Z=0)|$ is the circular velocity of the disc measured on the plane of the galaxy. The velocity distribution, $F(v)$, is assumed to be isotropic and Maxwellian, for simplicity

$$F(< v_{\rm rel,i}) = {\rm erf}(X_i) - \frac{2X_i}{\sqrt{\pi}} \exp[-X_i^2]; \tag{A.5}$$

where the term $X_i = |v_{\rm rel,i}|/\sqrt{2}\sigma_i$ is the one-dimensional velocity dispersion[14].

Chandrasekhar's formula was calculated for a massive point particle, but several authors showed that it can be applied to calculate the drag force on an extended satellite by adjusting appropriately the Coulomb logarithms (e.g., Colpi, Mayer & Governato 1999). Their choice is not trivial. Usually Λ is defined as $\Lambda = b_{max}/b_{min}$, where b_{max} is set to the typical scale of the system, and $b_{min} \equiv G(M_{\rm sat} + m)/V^2$, m being the mass of the background particles and V the typical velocity of the encounter, is the minimum impact parameter. A different definition is used for an extended satellite (Quinn & Goodman 1986).

The uncertainty in Λ_d and Λ_h directly reflects on that of the orbital decay rates, since the latters depend on the values of the Coulomb logarithms. A way to reduce such discrepancy is to treat $\ln\Lambda_h$ and $\ln\Lambda_d$ as free parameters. The self-consistent value of the Coulomb logarithm best fitting N-body orbits is $\ln\Lambda_h = 2.1$ (Peñarrubia, Just & Kroupa 2004; Arena & Bertin 2007), while TB01 and P10 adopt $\ln\Lambda_d = 0.5$. One should also make a correction to the expression for the disc friction, since the model assumed a constant satellite wake, and this approximation could reveal incorrect if the background density changes over small scales (e.g., when the satellite is in the disc plane). This can be corrected by smoothing the disc density (see Sec. 2.2.1 of TB01).

A.2 Mass loss

A finite size satellite moving through the host galaxy is expected to loose mass because of tidal stripping. The mass decrease of the satellite affects its dynamic, since the dynamical friction force expression contains $M^2_{\rm sat}$. It is clear that we need to estimate the mass loss in order to correctly describe the satellite motion. The loss of mass is due to the action of tidal forces. We distinguish two model behaviours: if the system is "slowly varying", we consider the material outside a limiting radius, dubbed "tidal radius", to be stripped, while if the system is "rapidly varying", the satellite material will be heated.

In the first case, one estimates the tidal radius as the distance, measured from the centre of the satellite, where the tidal force balances the satellite's self-gravity. In the case of satellites on circular orbits, the tidal radius is given by

$$R_t \approx \left(\frac{GM_{sat}}{\omega^2 - {\rm d}^2\Phi_{\rm h}/{\rm dr}^2}\right)^{1/3}; \tag{A.6}$$

(King 1962), where, as before, M_{sat} is the mass of the satellite ω is its angular velocity, and Φ_h is the host halo potential. Eq. (A.6) is valid if $M_{sat} << M_h$, $R_t << R_{system}$, and the satellite is corotating at ω. Eq. (A.6) describes a steady state loss of mass, while the mass changes on a general orbit should depend on the orbital period. One then assumes that mass beyond the tidal radius is lost in an orbital period.

[14]The velocity dispersion is defined as $\sigma_i(r) \equiv 1/\rho_i(r) \int_\infty^r \rho_i(r')[f_h(r') + f_d(r')]dr'$.

The calculation of $\mathrm{d}^2\Phi_h/\mathrm{d}r^2$ is performed averaging over the asphericity of the potential originated by the disc component, as follows

$$\frac{\mathrm{d}^2\Phi_h}{\mathrm{d}r^2} = \frac{\mathrm{d}}{\mathrm{d}r}\left(\frac{-GM(<r)}{r^2}\right) . \tag{A.7}$$

In real systems, satellites are not spherical and do not move inside spherically symmetric potentials. In such cases, Eq. (A.6) can be used to define an instantaneous tidal radius.

The stripping condition can be written in terms of the densities as,

$$\overline{\rho}_{\rm sat}(<R_{\rm t}) = \xi\overline{\rho}_{\rm gal}(<r) . \tag{A.8}$$

The previous equation localises the tidal limit at the radius beyond which the satellite mean density, $\overline{\rho}_{\rm sat}$, is larger by a factor ξ than the average galaxy density inside that radius r, where

$$\xi \equiv \frac{\overline{\rho}_{\rm sat}(<R_{\rm t})}{\overline{\rho}_{\rm gal}(<r)} = \left(\frac{r^3}{GM(<r)}\right)\left(\omega^2 - \frac{\mathrm{d}^2\Phi_h}{\mathrm{d}r^2}\right) \tag{A.9}$$

being ω the instantaneous angular velocity of the satellite and ω_c is the angular velocity of a circular orbit of radius r.

From the previous discussion, we can define an algorithm to calculate stripping.
1) We divide the orbital path of the satellite in discrete sections, and calculate the tidal radius through Eq. (A.8).
2) A fraction $\Delta t/t_{orb}$[15], of the material outside the virial radius will be removed.
3) Whereas in TB01, the satellite was considered disrupted when the tidal radius was smaller than the profile core radius, in our case, we define some other disruption criteria in Sect. 2.3.

A.3 Tidal Heating

As previously discussed, in the case of a rapidly varying gravitational potential, shocks are produced which result in changes in the satellite structure and give rise to an acceleration of the mass loss (e.g., Gnedin & Ostriker 1997, 1999; Gnedin, Hernquist & Ostriker 1999). A simple first order correction for tidal heating can be obtained as follows. Rapid shocks are identified by comparing the orbital period of the satellite, $t_{\rm orb,sat}$[16], with the disc shock timescale, $t_{\rm shock,d} = Z/V_{Z,\rm sat}$. If $t_{\rm shock,d} < t_{\rm orb,sat}$ the satellite is heated. We then calculate the change in energy, and the subsequent mass loss in the satellite. The energy change is obtained adopting the impulse approximation (Gnedin, Hernquist, & Ostriker 1999), which yields the velocity change produced by the tidal field in the encounter, relative to the centre of the satellite.

This velocity change produced in an encounter of duration t, for an element of unit mass located at $\mathbf{x}$ with respect to the centre of the satellite, writes

$$\Delta\mathbf{V} = \int_0^t \mathbf{A}_{\rm tid}(t')dt', \tag{A.10}$$

where the term $\mathbf{A}_{\rm tid}$ is the tidal acceleration.

[15] Δt is the timestep, while $t_{orb} = 2\pi/\omega$ is the orbital period, which is assumed to be the typical time-scale for the mass loss of the satellite.

[16] $t_{\rm orb,sat} = 2\pi r_{\rm h}/V_c(r_{\rm h})$ is the satellite orbital period at its half-mass radius, r_h.

The first order change in energy is given by

$$\Delta E_1(t) = W_{\rm tid}(t) = \frac{1}{2}\Delta V^2 \tag{A.11}$$

We divide the shock in n time steps of length Δt and suppose that the satellite is sufficiently small so that the tidal acceleration can be expressed in terms of the gradient of the gravitational acceleration produced by the external potential, $\mathbf{g}$. We then average the change of energy on a sphere of radius r, in a time step, as

$$\begin{aligned}
&\Delta W_{\rm tid}(t_n \rightarrow t_{n+1}) \\
&= \frac{1}{6}\, r^2\, \Delta t^2 \left[2\, g_{a,b}(t_n) \sum_{i=0}^{n-1} g_{a,b}(t_i) \right. \\
&\qquad \left. + \quad g_{a,b}(t_n) g_{a,b}(t_n) \right]
\end{aligned} \tag{A.12}$$

where $g_{a,b} = \partial g_a / \partial x_b$ is evaluated at $\mathbf{x} = 0$[17].

The impulse approximation, upon which the calculation of Eq. (A.12) is based, breaks down in the central part of the satellite where the dynamical time-scales can be comparable to, or even shorter than, the duration of the shock. When this happens the shock effects are significantly reduced.

This is taken into account through a first-order adiabatic correction (Gnedin & Ostriker 1999)

$$\Delta E_1 = A_1(x) \Delta E_{1,\rm imp} \ , \tag{A.13}$$

where $x = t_{\rm shock}/t_{\rm orb,sat}$ is the adiabatic parameter, and $A_1(x) = (1+x^2)^{-\beta}$, with $\beta = 5/2$ (Gnedin & Ostriker 1999).

Another correction required is connected to the satellite internal dispersion velocity, which is altered by heating (Kundić & Ostriker 1995). We start by computing the energy changes at first-order and further take into account the higher order effects through the heating coefficient, $\epsilon_{\rm h}$, as

$$\Delta E = \epsilon_{\rm h} \Delta E_1 = \epsilon_{\rm h} A_1(x) \Delta E_{1,imp} = \epsilon_{\rm h} A_1(x) \delta W_{tid}. \tag{A.14}$$

Gnedin & Ostriker (1997) estimated $\epsilon_{\rm h} \simeq 7/3$.

In this paper, we follow TB01 in adopting the value $\epsilon_{\rm h} = 3$.

Practical determination of the effect of heating on the satellite leads us to assume for each mass element that its potential energy is proportional to its total energy. We note that shell crossing is not taken into account by the mass distribution changes.

Consequently, we write that a mass element will have a total energy $E(r)$ proportional to $-1/r$, and a radius change $\Delta r \propto \Delta E(r)\ r^2$.

Inside radius r the mean density will change as

$$\Delta \overline{\rho}_r = \ \Delta \left(\frac{3M(<r)}{4\pi r^3} \right) \ \propto -\frac{\Delta r}{r^4} \propto -\frac{\Delta E(r)}{r^2} \ . \tag{A.15}$$

The previous equation shows how the bound mass density in the satellite can decrease because of heating, with the results of an acceleration of the mass loss. The decrease in

[17] These equations and several others were solved using the ABS method (Spedicato et al. 2003)

density can correspond to, either an increase of the velocity dispersion in, or an expansion of, the satellite. In any case, it gives rise to the same change in the bound mass.

We can calculate the density change due to tidal heating, at a radius r as a function of time. Applying then the equation for tidal stripping, (Eq. A.8), to the heated density we can estimate the quantity of mass lost.

In the calculation, we smoothed the disc mass in the vertical direction, as already mentioned, over twice the disc scale height. We assume the velocity dispersion of the disc to read as

$$\sigma_{\rm h} = (V_{\rm c,h}^2)^{1/2}/\sqrt{2},$$

and

$$\sigma_{\rm d} = V_{\rm c,d}/\sqrt{2} = \sigma_{\rm o} \exp(-R/R_{\rm o})$$

where $V_{\rm c,h}$, is the circular velocity of the halo, and $V_{\rm c,d}$ that of the disc. $\sigma_{\rm o}$ is set to 143 km/s and $R_{\rm o}$ to 7kpc (namely $2\,R_{\rm d}$), in agreement with Velazquez & White (1999).

The model depends on three parameters: $\ln \Lambda_{\rm h}$ (strongest dependence), $\epsilon_{\rm h}$ (weaker than the previous), and $\ln \Lambda_{\rm d}$ (weak dependence). To evaluate the sensitivity of the results to parameter variations, 20% changes in the second parameter ($\epsilon_{\rm h}$) were issued: even with such modulations, only slight changes to the results were produced.